Results: For GTVs the median DICEs were 0.88 and 0.63 for RH and H, respectively, while for parotid gland were 0.94 and 0.82, and for spinal cord were 0.94 and 0.88, respectively. Although dose differences on GTVs show the median variations within 1% with minimal values up to 8%, TCP values were 63.7%, 69.7% and 61.9 % for planned, RH and H approach, respectively. Moreover, the average NTCP for homo-lateral parotids it was 36 %, 46 % and 34 %; while for contra-lateral parotids was 28%, 36% and 27% based on planned, RH-based and H-based accumulated DVHs, respectively.

Conclusion: RH strategy generates structures well in agreement with ones manually contoured, supporting the goodness of generated deformation matrix, resulting an appropriate strategy to perform dose tracking in HN cancer patients eligible for ART. Home-made tools/routine, as developed in this work, are mandatory to evaluated results and permit the adoption of a dose tracking strategy.

EP-1825

Delivered dose determination in large organ deformations: Pre-requirement for adaptive RT for LACC.

P.V. Nguyen[1], F. Lakosi[1], J. Hermesse[1], S. Nicolas[1], A. Cifor[2], M. Gooding[2], P.A. Coucke[1], T. Kadir[2], A. Gulyban[1]
[1]*C.H.U. - Sart Tilman, Radiotherapy Department, Liège, Belgium*
[2]*Mirada Medical Ltd, Physics, Oxford, United Kingdom*

Purpose or Objective: To create robust methodology for accumulating delivered dose to organs on the basis of daily cone beam computer tomography (CBCT) images using Radial Basis Function with Robust Point Matching (RBF-RPM) deformation algorithm. Clinical evaluation includes clinical target volume (CTV) coverage for patient with locally advanced cervical cancer (LACC).

Material and Methods: Between June and September 2015 five consecutive LACC patients were scanned with empty and full bladder conditions for treatment planning purposes. Primary CTV was delineated in both scans creating an internal target volume (ITV) concept and the distance between the tip of the uterus was measured. Primary ITV and lymph node CTVs were expanded with 10 mm margin to generate the planning target volume (PTV). Advanced treatment planning technique (VMAT or IMRT) were used for delivering a total dose of 45 Gy in 25 fractions with daily online correction CBCT. On every CBCT the 1) current position of the primary CTV were delineated and 2) the planned dose matrix were co-registered and eventually transposed to CBCT rigidly. Using the Mirada RTx (version 1.6.2, Mirada Medical, Oxford, United Kingdom) between the planning reference CT (= full bladder) and each CBCT a "CTV-guided" deformation (using the RBF-RPM algorithm) matrix were generated to deform the dose matrices from CBCT to the planning CT. The dose parameters on the initial CTV were evaluated on a single fraction basis (worst and average) and summed dose basis compared to the reference plan value.

Results: The average tip movement of the uterus was 2.2 cm (range 0.5-5.7 cm). A total of 118 CBCTs were eligible to perform the CTV delineation and the dose matrix transformation (rigid CT to CBCT, deformation CBCT to CT). Visual verification of each individual deformation grid were considered as clinically plausible and smooth (Figure 1). The changes in CTV_V95% were -4.7% (range [-7.0,-3.62], -0.3% [-1.4, 2.2] for the single fraction worst and mean, while for the summed actual delivery -0.6% [-3.7, 1.76]. Deviation of CTV_D95% resulted in -2.7 Gy [-5.8, -1.1] and -0.4 Gy [-0.9, -0.2] for the single fraction worst and mean, while for the summed actual delivery -0.5 Gy [-2.1, 0.1].

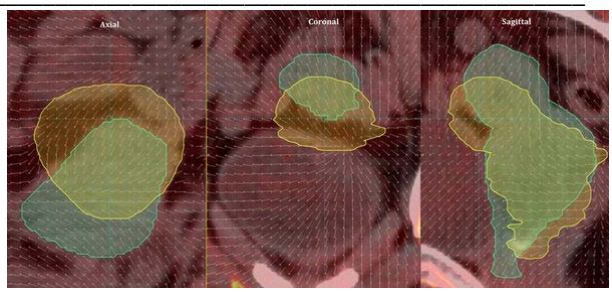

Conclusion: Using VMAT/IMRT for LACC treatment in combination with ITV concept and 10 mm margin provides a safe treatment option in the presence of large daily organ deformation. The dose accumulation using the RBF-RPM algorithm is feasible and provides a powerful tool to evaluate delivered dose not only to CTV but also to organs at risk. This methodology allows an environment to test various adaptive strategies (e.g. library of plans based LACC radiotherapy) and CTV to PTV margins in a safe retrospective manner.

Electronic Poster: Physics track: CT Imaging for treatment preparation

EP-1826

An empirical post-reconstruction method for beam hardening correction in CT reconstruction

B. Yang[1], H. Geng[1], W.W. Lam[1], K.Y. Cheung[1], S.K. Yu[1]
[1]*Hong Kong Sanatorium & Hospital, Medical Physics and Research Department, Happy Valley, Hong Kong SAR China*

Purpose or Objective: Beam hardening artifacts in X-ray computed tomography is caused by the polyenergetic spectrum of X-ray source. In this abstract we describe an empirical post-reconstruction method which removes the artifacts successfully.

Material and Methods: Our proposed post-reconstruction method has similar approach as a well-known correction method first developed by Joseph and Spital (J&S). Our method also requires prior knowledge of the X-ray spectrum and consists of three stages of correction. The first step is a so-called soft tissue correction which determines the equivalent length of soft tissue Te by solving the non-linear equation:

$Pi=\sum\omega\exp(-\mu(s)\rho(s)Te)$

In the second step, this image is segmented into soft tissue Ts and high density Tb (e.g. bone) region by setting a threshold. Different from J&S, we consider $\mu(s)\rho(s)Tb$ as part of the density map of high density region and calculate the projection data:

$Bi=\sum\omega\exp(-\mu(b)\mu(s)\rho(s)Tb)$

The third step applies the soft tissue correction again by solving the non-linear equation:

$\exp(-\ln(Pi)+\ln(Bi))=\sum\omega\exp(\mu(s)\rho(s)Ts)$

, therefore a density map $\rho(s)Ts$ is reconstructed. The final image will be the sum of $\rho(s)Ts$ and $\rho(s)Tb$. We created a 128 x 128 pixel numerical phantom which was a circular phantom consisting of water, four small regions containing bone and a small region containing fat. For validating the robustness of the method, we also replaced the four small regions with those containing aluminum and titanium. The projection data consisted of 140 radial samples and 100 angular samples over 180 degree from a 100 kVp parallel X-ray beam.

Results: The results of the post-reconstruction method for the phantom containing bone, aluminum and titanium are shown respectively. Within each figure, top left is the true phantom image; the middle is the direct filtered back projection (FBP) result with no correction; the top right is the post-reconstruction result; the profile plot is sampled at the center of phantom. For the cases of bone and aluminum, the beam hardening artifacts are removed successfully. Even in the most challenging case of titanium, the artifacts are suppressed greatly. Compared with the results using method from J&S, the density values of reconstructed high density

region are closer to the real values with deviation +5.3%, +0.4% and +10.2% for bone, aluminum and titanium respectively.

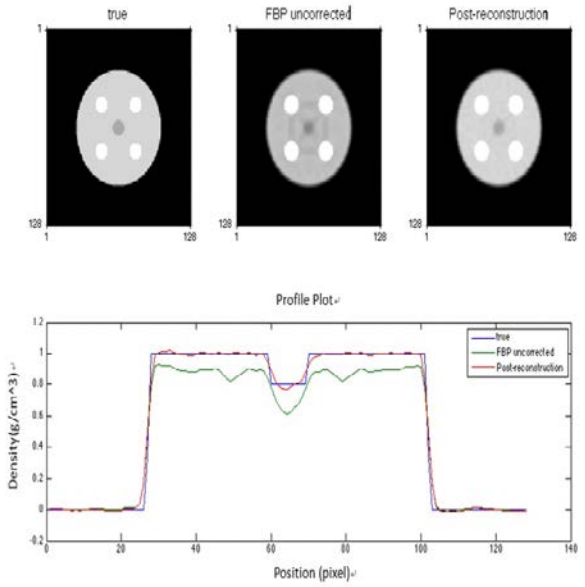

Figure 1 Results of phantom containing aluminum.

Conclusion: Our proposed empirical post-reconstruction method works well in beam hardening correction.

EP-1827

Dual energy Computed Tomography based tissue characterisation for Radiotherapy treatment planning

N. Tomic[1], H. Bekerat[1], F. DeBlois[1], J. Seuntjens[2], R. Forghani[3], S. Devic[2]

[1]*Jewish General Hospital, Radiation Oncology, Montreal, Canada*

[2]*McGill University, Oncology, Montreal, Canada*

[3]*Jewish General Hospital, Diagnostic Radiology, Montreal, Canada*

Purpose or Objective: It is known that both kVp settings, as well as geometric distribution of various materials, lead to significant change of the HU values, being the largest for high-Z materials and lowest kVp setting used for CT scanning. On the other hand, it is well known that dose distributions around low-energy brachytherapy sources (103Pd, 125I) are highly dependent on the architecture and composition of tissue heterogeneities in and around the implant. Both measurements and Monte Carlo calculations show that the errors caused by improper tissue characterization are around 10% for higher energy sources and significantly higher for low energy sources. We investigated the ability of dual-energy CT (DECT) to characterize more accurately tissue composition.

Material and Methods: Figure 1.a shows the RMI-467 heterogeneity phantom scanned in DECT mode with 3 different setups: the first set-up in which we placed high electron density (ED) plugs within the outer ring of the phantom is called Normal one, as we assume that in clinical practice this would be the most commonly used geometrical distribution of tissue ED plugs. In the second set-up we arranged high ED plugs within the inner ring and in the third one, ED plugs were randomly distributed. All three setups were scanned with the same DECT technique using a single-source DECT scanner with fast kVp switching (Discovery CT750HD; GE Healthcare). Images were reconstructed into 1.25-mm slices with a 40-cm display field of view and a 512 X 512 matrix and transferred to a GE Advantage workstation for advanced DECT analysis. Spectral Hounsfield unit curves (SHUACs) were then generated from 50 to 140-keV, in 10-keV increments, for each tissue equivalent plug.

Results: Figures 1.b-d represents HU to ED calibration curves for monochromatic CT images at 50, 80 and 140 keV respectively. As expected, the dynamic range of HU shrinks with increased photon energy as the attenuation coefficient ranges decrease. The same figures also suggest that the spread of HUs for the three different geometrical setups is the smallest at 80 keV. To quantify variation in HUs with photon energy, we calculated relative variation for various tissue equivalent materials (LN 450 Lung, Breast, Liver, CB2-30%, CB2-50%, Cortical Bone) and plotted for several different photon energies in Fig.1.e.

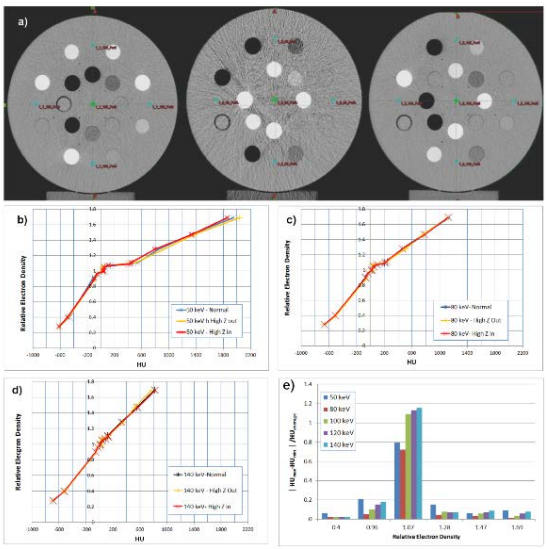

Figure 1 Impact of electron density spatial distribution on reconstructed Hounsfield Units on virtual monochromatic DECT images: a) three experimental setup (left – high Z material plugs in outer ring; center – high Z plugs in inner ring; right – standard random plug distribution); b-d) HU-ED curves for three different experimental setups at 50 keV, 80 keV and 140 keV respectively; e) relative variation of the reconstructed HUs for various materials taken from different reconstructed virtual monochromatic energy images.

Conclusion: Spectral Hounsfield unit curves demonstrate the lowest HU variation at 80 keV for the three different geometries used in this work. Among all the energies and all materials presented, the largest difference appears at high Z tissue equivalent plugs. This suggests that 80 keV virtual monochromatic DECT reconstructions may enable more accurate dose calculations at both megavoltage and kilo-voltage photon energies.

EP-1828

Liver SBRT: benefits from breath-triggered MRI in treatment position for accurate lesion contouring

L. Parent[1], A. Tournier[1], M. Rives[2], F. Izar[2], R. Aziza[3], Y. Sekkal[3], N. Morel[3], S. Ken[1]

[1]*Institut Universitaire du Cancer Toulouse Oncopôle, Engineering and Medical Physics Department, Toulouse, France*

[2]*Institut Universitaire du Cancer Toulouse Oncopôle, Radiotherapy Department, Toulouse, France*

[3]*Institut Universitaire du Cancer Toulouse Oncopôle, Imaging Department, Toulouse, France*

Purpose or Objective: As part of the stereotactic body radiotherapy (SBRT) program in our institution, magnetic resonance imaging (MRI) acquisition in treatment position for the liver was implemented. Significant liver motion can be observed due to breathing motion. The aim of this study is to report the benefits of setting out a time-correlated and breath-triggered MRI protocol optimized for radiotherapy (RT) planning in order to account for liver breathing motion.

Material and Methods: Prior to imaging, three internal gold fiducials were implanted under echo or CT guidance in the vicinity of the lesion site in order to improve images registration, patient's positioning and target volume tracking during treatment.

A 4D CT scan was acquired on a GE Healthcare Optima CT580 RT. Patient immobilization and positioning was set up with